Flame/Turbulence Interactions in Premixed Stagnating Flows

Thomas M. Smith *
Parallel Computational Sciences Dept.
Sandia National Laboratories
Abuquerque, NM 87185
and
Suresh Menon †
School of Aerospace Engineering
Georgia Institute of Technology
Atlanta, Georgia 30332-0150

Unsteady simulations of stagnation point flames are conducted in order to study flame turbulence interactions in a relatively simple flow environment. Flame propagation is represented using a flamelet model called the G equation. Two subgrid models are used to close the filtered G equation. The effects of significant heat release on the turbulent flow and the effect of varying turbulence intensity on the flame structure have been studied. The results show that at low turbulence intensities, the heat release dramatically alters the flow field and as the intensity is increased, heat release has a dimishing effect. The turbulent flame speeds are also shown to be in reasonable quantitative agreement with experimental data.

Introduction

Understanding flame/turbulence interactions in reacting turbulent flows even in simple flow configurations is a critical component in the development of predictive modeling capabilities. Chemistry and turbulence interactions involve a wide range of length and time scales that vary locally. The enhancement of mixing and burning rates by highly fluctuating rotational flow and the augmentation of the hydrodynamic field by heat release are dynamic and local phenomena. In low intensity turbulence (low u'/S_L, where u' is the turbulence intensity and S_L is the laminar flame speed) and high product to reactant temperature ratios (T_p/T_f, where T is the temperature and p and f denote product and fuel respectively), preferential acceleration of light product gases gives rise to counter-gradient diffusion (Cho *et al.*, 1988; Bray, 1995 and Veynante *et al.*, 1997) while at high u'/S_L and moderate temperature ratios, gradient diffusion is observed through most of the flame brush. Dilatation caused by heat release and increased viscous effects act on the fluctuating velocity field and reduce the intensity behind the flame front. However, baroclinic torque which is produced when the pressure and density gradients are not aligned is a source of turbulence production (McMurtry *et. al*, 1989 and Bray, 1995).

Because flame/turbulence interactions are dynamic and transient, steady state approaches for predicting flame/turbulence interactions are limited. This problem may be solved in theory by direct numerical simulation (DNS), where all length and time scales are directly computed, however, DNS is restricted to computing only a narrow band of length and time scales due to available computational resource limitations.

Large-Eddy simulation (LES) is an emerging technology that bridges the gap between (DNS) and the Reynolds Averaged Navier-Stokes (RANS) steady state approach. In LES, the large scales are directly computed and the effect of the small scales on the large scales is modeled. In LES the majority of transport phenomena is computed directly compared to RANS where all turbulent transport is modeled.

In two earlier papers (Smith and Menon, 1997, 1998) the computational methodology for simulating stagnation point flames was described. This included boundary conditions and unsteady inflow velocity forcing. In those studies, the flame propagation was described using two approaches. The first approach was the well known G field equation (Kerstein *et al.* 1988) for flame propagation and the second was a subgrid modeling approach based on the Linear-Eddy Model (Kerstein, 1991; Kerstein, 1986; and Menon and Kerstein, 1992). Some important features of the second methodology include: appropriate characterization of fine-scale flame wrinkling, flamelet burning and transport of the progress variable by the resolved scale turbulence without using gradient diffusion models.

In reacting flows where the turbulence scales are

*Post Doctoral Fellow, Student Member, AIAA
†Professor, Senior Member, AIAA

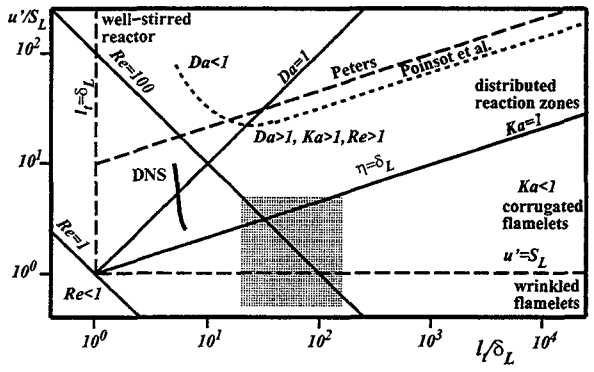

Fig. 1 Turbulent combustion diagram.

large in comparison to the combustion scales (*i.e.*, the flame thickness) flamelet theory is justified to describe the interactions between the combustion processes and the hydrodynamic processes. Therefore, flamelet models may be used to describe large resolved scale interactions.

In this paper, flame/turbulence interactions in stagnation point flows will be studied within the context of the flamelet propagation discussed above. Using this approach and changing the physical parameter (u'/S_L), the capabilities of this approach will be evaluated.

Stagnation point flames have several advantages that are exploited in order to evaluate this modeling approach. First, the flow is unsteady and stationary and, thus, the flame position and the propagation rates are steady and fully developed. The steady nature of these flows allows for statistical properties to be analyzed. Second, the turbulence is shear free and nearly homogeneous which is the simplest to analyze. Finally, the flame front is planar with the mean direction normal to the oncoming reactant flow.

The turbulent combustion diagram is presented in Fig. 1. A review of the different regimes of combustion is given by Peters (1986). Regimes of premixed combustion are defined in terms of characteristic velocity and length scales and three parameters: Reynolds number, Damköhler number and Karlovitz number. Flamelets are expected to exist in the region below $Ka = 1$. However, recent studies have argued that flamelets exist well above this limit (Poinsot *et. al*, 1990; Peters, 1997; and Roberts *et. al*, 1993). On this plot is shown the region where the majority of turbulent stagnation point flames have been studied. It can be seen that stagnation point flames predomenantly exist in the flamelet regime.

Large-Eddy Simulation of Reacting Flows

A conceptual picture that compares the resolved LES flame front to the actual flame front is presented in Fig. 2. Because the actual flame thickness is much smaller than the LES computational grid, structural

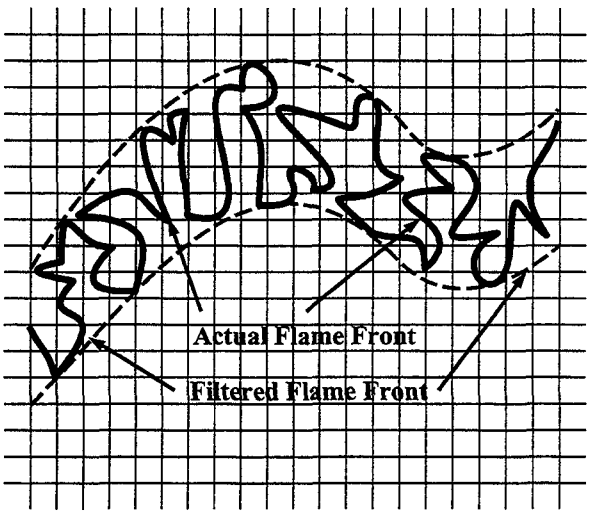

Fig. 2 Conceptual diagram showing the LES resolved flame front and the acutual flame front.

information that influences the rate of propagation is lost. Three mechanisms of propagation arise when the actual flame front is represented by the filtered flame front. These are: unresolved transport of the flame by turbulent stirring, unresolved flame area and the local response to flame stretch. This information must be modeled in order to regain the original flame propagation.

The equations of LES are the mass weighted spatially filtered mass, momentum, energy, and species equations. Subgrid transport terms arise as a result of filtering nonlinear terms in the equations and models must be found for them. Of particular interest is the filtered species equation which contains a subgrid flux that is due to the unresolved turbulent velocity field and the mean reaction rate. Both of these unknown terms are troublesome. The subgrid flux $\bar{\rho}[\widetilde{u_i Y_k} - \tilde{u}_i \tilde{Y}_k]$ is the transport of species mass fraction by subgrid scale turbulence and is responsible for enhancing micro-scale mixing. The mean reaction rate $\bar{\omega}_k$ depends on correlations between resolved and unresolved temperature $(\tilde{T},\ T")$, and species $(\tilde{Y}_k,\ Y_k")$ correlations and is very difficult to evaluate.

The current approach replaces the filtered species equations with a conventional flamelet model referred to as the G equation described in the following section.

G-Equation Flamelet Model

The flamelet assumption describes a regime in premixed combustion that is often encountered in practical combustion devices. Within the flamelet assumption, the flame thickness (δ_l) is small compared to the smallest dynamic scale of turbulence $(\eta$, the Kolmogorov scale) and the characteristic burning time (τ_c) is small compared to the characteristic flow time (τ). As a result, the flame structure remains unaltered and the flame can be considered a thin front propagating at a speed dictated by the mixture properties that

is wrinkled and convected by the flow. A model equation that describes the propagation of a thin flame by convective transport and normal burning (self propagation by Huygens' principle) has been introduced called the *G-field* equation (Williams, 1985; Kerstein *et al.*, 1988)

$$\frac{\partial G}{\partial t} + \mathbf{u} \cdot \nabla G = S_L |\nabla G| \tag{1}$$

where G is a progress variable that defines the location of the flame, $\mathbf{u}$ is the mass averaged velocity vector and S_L is the local laminar flame speed. Eq. (1) describes the convection of a level surface, defined as $G = G_o$, by the fluid velocity while simultaneously undergoing propagation normal to itself at a speed S_L according to Huygens' principle. In the flow field, the value of G is in the range [0,1] and in flame front modeling, G exhibits a step function like behavior, separating the burnt region ($G < G_o$) from the unburned region ($G > G_o$). G is assigned the value of unity in the unburned region and zero in the burnt region with the thin flame identified by a fixed value of $0 < G_o < 1$. In the finite-volume numerical approach, an equivalent equation is written

$$\frac{\partial \rho G}{\partial t} + \nabla \cdot \rho \mathbf{u} G = \rho_o S_L^o |\nabla G| \tag{2}$$

where ρ_o is the reference reactant density and S_L^o is the undisturbed laminar flame speed. The relationship, $\rho_o S_L^o = \rho S_L$ is an expression of mass conservation through the flame.

Upon filtering

$$\frac{\partial \bar{\rho} \tilde{G}}{\partial t} + \nabla \cdot \bar{\rho} \tilde{\mathbf{u}} \tilde{G} = \overline{\rho_o S_L^o |\nabla G|} - \nabla \cdot (\bar{\rho}[\widetilde{\mathbf{u}G} - \tilde{\mathbf{u}}\tilde{G}]). \tag{3}$$

The unresolved transport term is modeled using a gradient assumption (Im, 1995; Im *et al.*, 1997; Piana *et al.*, 1997, and Veynante and Poinsot 1997a)

$$\bar{\rho}[\widetilde{\mathbf{u}G} - \tilde{\mathbf{u}}\tilde{G}] \approx -\frac{\mu_t}{Sc^G} \nabla \tilde{G} \tag{4}$$

where μ_t is an eddy viscosity and Sc^G is a Schmidt number. At first glance, the gradient closure approximation appears to clearly violate the physics of turbulent transport given that counter-gradient diffusion dominates the transport of scalar fluxes in many situations. However, it must be kept in mind that counter-gradient transport is a large scale phenomena (Bray, 1995) and in the LES methodology, the large scales are directly computed and therefore, counter-gradient diffusion should be accounted for despite the subgrid closure assumed. This, of course, will require evaluation. In addition, counter-gradient diffusion is produced by the preferential acceleration of lighter parcels of fluid as opposed to heavier parcels by the mean pressure gradient. Given the current subgrid modeling technology, pressure gradient effects are not included in the closure models and therefore the ability to produce counter-gradient diffusion is absent from all models that neglect pressure effects.

For closure of the source term, Yakhot's RNG model is used (Yakhot, 1988; Menon and Jou, 1991). This model is an analytical expression for the turbulent flame speed as a function of turbulence intensity ($u_t/S_L = exp[u'^2/u_t^2]$) obtained from Eq. (1). For flamelet combustion, $\frac{A_t}{A_l} = \frac{u_t}{S_L}$, where A_t and A_l are the turbulent and laminar flame areas respectively, and therefore Yakhot's model is an estimate of the flame wrinkling due to the turbulence intensity. Therefore, in the LES context, the propagation rate is no longer $\rho_o S_L^o$ but is instead replaced by $\rho_o u_f$ where u_f is obtained from $(u_f/S_L = exp[(u'_{sgs})^2/(u_f)^2])$ which is the subgrid turbulent burning rate that accounts for unresolved flame wrinkling. The turbulence intensity appearing in the turbulent flame speed model is the subgrid turbulence intensity, $u'_{sgs} = \sqrt{\frac{2}{3} k^{sgs}}$ where k^{sgs} is the subgrid turbulent kinetic energy given by, $k^{sgs} = \frac{1}{2}[\widetilde{u_l u_l} - \tilde{u}_l \tilde{u}_l]$. Note that $u'_{sgs} \neq u''_i$ which represents the fluctuating part of u_i. A model equation for the subgrid turbulent kinetic energy is discussed in Smith and Menon (1997). It was argued there that in two-dimensional constant flame speed simulations, the subgrid kinetic energy is negligible and therefore, subgrid closure terms can be neglected. In the present study, the subgrid terms are included and the subgrid turbulence intensity is retained to provide a measure of the subgrid flame speed through Yakhot's model.

This model assumes that the flame is a thin sheet having no internal structure and, therefore, is applicable only in the flamelet combustion regime. Furthermore, it does not take into account flame stretching effects and so cannot predict extinction. However, it has been shown that the model compares well with experimental data in the low to moderately high u'/S_L range and also predicts (in reasonable agreement with data) a rapid increase in u_t/S_L at low u'/S_L and then a *bending* slope at high u'/S_L (Yakhot, 1988). The source term for the filtered G equation becomes

$$\overline{\rho_o S_L^o |\nabla G|} \approx \rho_o u_t |\nabla \tilde{G}|. \tag{5}$$

In summary the flamelet model just proposed addresses two of the three major issues in LES, namely the unresolved scalar transport and the increased burning rate do to flame wrinkling. What has not been addressed is the local response due to flame stretch.

Thermodynamic coupling is through the internal energy $\tilde{e} = c_v \tilde{T} + \Delta h_f \tilde{G}$, where $\Delta h_f = c_p(T_p - T_f)$ is the heat of formation, c_v and c_p are the specific heats at constant volume and pressure respectively. In this case Δh_f should be a heavy side function of G, however, this produces a numerical instability when the flame front is steeply varying. Menon (1991) has pointed

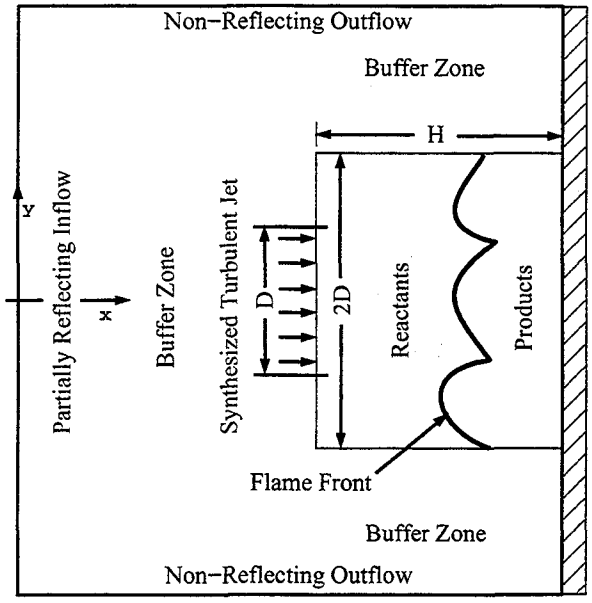

Fig. 3 Schematic diagram of the stagnation point flame simulation computational domain.

out that the linear dependence on $\tilde{G}$ results in a distributed heat release that tracks the flame and does not cause significant error as long as the front is not a broad front. In addition this assumption must be viewed as more realistic than constant density approximations.

Simulation of Stagnation Point Flames

The numerical simulations of stagnation point flames were designed to mimic the experiments of Cho *et al.* (1986), Cho *et al.* (1988), and Liu and Lenze (1988) while reducing the complexity by simplifying inflow and wall boundary conditions. A schematic diagram of the computational domain is presented in Fig. 3. A buffer region (that numerically suppresses unsteady physical fluctuations by stretching the computational grid spacing) surrounds the core grid mesh on three sides of the two-dimensional domain. A jet of diameter D (0.05m) of premixed reactants is placed at a distance H away from a flat wall. The computational domain is tilted 90 degrees to that of the experimental apparatus so the flow is from left to right, the wall is along the vertical direction and the outflow boundaries are normal to the y direction.

In the experiments, a co-flowing laminar jet surrounds the turbulent jet in order to prevent large scale entrainment from the ambient air. The computational co-flowing jet extends to the edge of the outflow boundary to prevent entrainment at the inflow boundary, a situation that is very difficult to handle because the boundary conditions are not easily specified.

Turbulence is generated by passing the premixed stream through a grid or a plate with holes, just prior to the converging nozzle. This produces a nearly uniform homogeneous turbulent stream. Synthesized turbulence which is nearly isotropic, divergence free, and non-periodic is generated from a specified turbulent kinetic energy spectrum and turbulence intensity in a manner similar to Lee *et al.* (1992). The synthesized turbulence is convected at the local mean axial velocity and is included using forcing functions in the governing momentum equations.

The width of the domain extends $2D$ parallel to the wall. The inflow boundary is at $41/3D$ ahead of the jet exit. The outflow boundaries are 5D away from the stagnation point (Smith and Menon, 1997, 1998). A slip adiabatic condition was imposed at the wall. This means that there is no boundary layer created as the flow passes over and parallel to the wall. It has been discussed in Cho *et al.* (1988) that the flame location is well outside of the thermal layer and they argue that it has no significant effect on the flame propagation. In addition, there is no significant boundary layer at the stagnation point because the transverse component of velocity is zero on the stagnation stream line. This argument is implicit in these simulations for it greatly reduces the computational cost by not requiring a refined mesh normal to the wall. Partially-reflecting characteristic based inflow boundary conditions were used (Smith and Menon, 1997, 1998). This set of boundary conditions greatly reduce the amplitude of the reflected pressure waves. Non-reflecting characteristic boundary conditions are imposed on the vertical outflow boundaries similar to those suggested by Poinsot and Lele (1992).

The governing equations with boundary conditions and associated subgrid models are solved using an explicit time marching MacCormack type finite-volume scheme that is formally second-order accurate in time and fourth-order accurate in space (Nelson and Menon, 1998). In the buffer regions of the domain, the order of the scheme has been reduced to second-order in space (which is known to be significantly more dissipative than fourth-order) in order to provide additional damping of oscillations. The code has been implemented with the MPI message passing language and runs on distributed memory parallel machines.

Results and Discussion

Four simulations were conducted with two different sets of physical parameters. These are listed in Table 1. In a previous study the temperature ratio and the turbulence intensity were varied. The earlier simulations provided information on how the heat release and turbulence intensity affect the flow field and turbulent flame structure. In this study only the turbulence intensity has been varied and the flame speed and distance to the wall are different than the previous studies (Smith and Menon 1998). The computational grid chosen was 180x300 with 96x128 points in the core grid region and 64 points were used to resolve the turbulent jet flow.

Table 1 Turbulent Stagnation Point Flame Properties.

Run	Rel	Da	U m/s	S_L m/s	T_p/T_f	u'/S_L	u_t/S_L
RS1	43	7	5	0.4	7	0.9	2.23
RS2	87	3.5	5	0.4	7	3.6	6.3

The mean jet velocity (U_o) was 5m/s and the integral length scale (l_t) was 0.0053 m (each l_t was resolved with approximately 6 grid cells). The "flame" G profile was resolved with 5 to 7 points making the effective $\delta_l \approx$ three to five mm (significantly higher than real flames). The integral scale increases in two-dimensional turbulence as it advances towards the wall so the flow resolution increases. However, the flame structure remains nearly constant in width. As a result the resolution of the flame remains nearly the same everywhere in the core region. The exception to this is when cusps arise which can be a concern using the G equation model with constant flame speed. Cusps create very high curvatures that can not be resolved. However, the present non-constant flame speed simulations combined with very energetic turbulence prevent cusps from becoming a problem.

Each simulation ran for at least a 1.5 million time steps requiring about 32 cpu hours using 64 nodes on a Cray T3E. This corresponds to roughly 80 large-eddy turnover times for flames RS2 and roughly 4.7 flow through times for all flames, where a flow through time is defined as $3D/U_o$. Statistics were generated from the final 80% of the data.

The Reynolds time averaged mean axial velocities from two simulations are shown in Fig. 4. In Fig. 4, the turbulence intensity has been varied for a constant heat release of $T_p/T_f = 7$. Note that the velocity decreases non-linearly at the jet exit and reaches a linear decay only near the wall. This is due to the zero divergence at the jet nozzle. For low u'/S_L, the acceleration in velocity through the flame is distinct. As u'/S_L increases and the flame normal direction becomes more random, reducing the mean acceleration. The increased burning rate of RS2 compared to RS1 is apparent by comparing the relative location of the local minimum in the time averaged profile. The local minimum for the higher u' case, is further from the wall indicating that reactants are being consumed faster than in the case of RS1.

The Reynolds time averaged r.m.s. axial velocity components are shown as a function of turbulence intensity holding the heat release constant in Fig. 5. The synthesized turbulence decays more rapidly than in experiments (Smith and Menon, 1998). The levels of u' and v' are similar in magnitude for RS1 approxmimating homogeneity, the magnitudes are significantly different in RS2, which is a very high intensity flow.

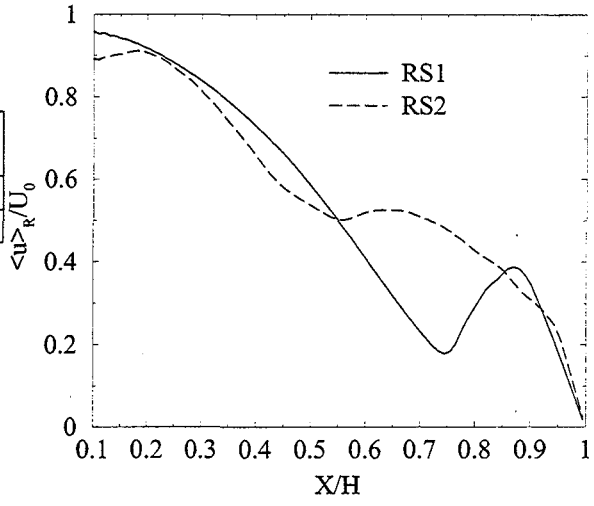

Fig. 4 Reynolds averaged axial velocity.

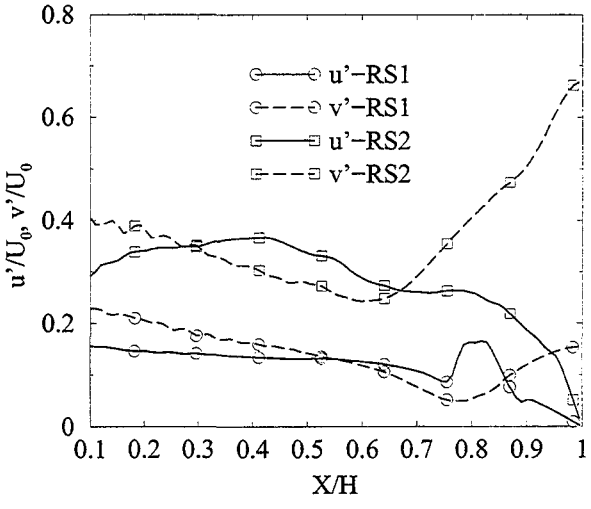

Fig. 5 Reynolds averaged r.m.s. axial and radial velocity components.

There is a noticeable increase in u' through the flame in RS1 that does not appear to be as strong in RS2. The higher intensity turbulence tends to homogenize the flow reducing the acceleration. In the post flame region, the velocity component decays to zero. In both simulations, v' increases through the flame. These accelerations have also been observed in experiments (Cho *et. al* 1996, 1998). However, due to the slip boundary condition imposed at the wall, v' does not decay to zero.

The relationship between the heat release and the propagation rate is clearly seen by comparing the average modulus of the gradient of G (Fig. 6) with the average velocity divergence in Fig. 7. The curves are very similar and vary mainly in magnitude. The magnitude is a function of the flame speed and the temperature ratios. The extent of the RS2 curves compared to the RS1 curves shows the relative comsumption rate to be higher for RS2.

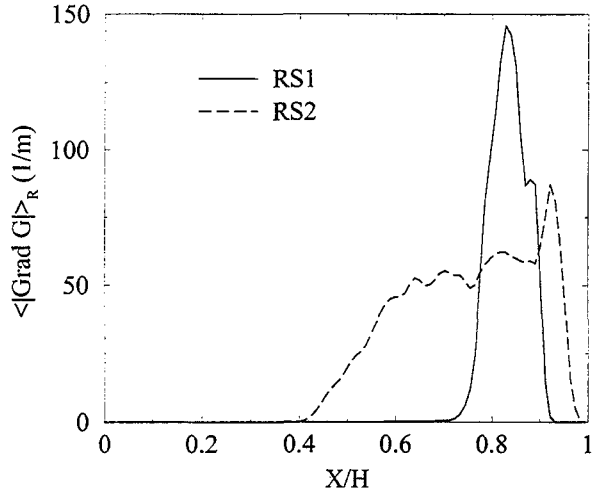

Fig. 6 Reynolds averaged modulus of the gradient of G.

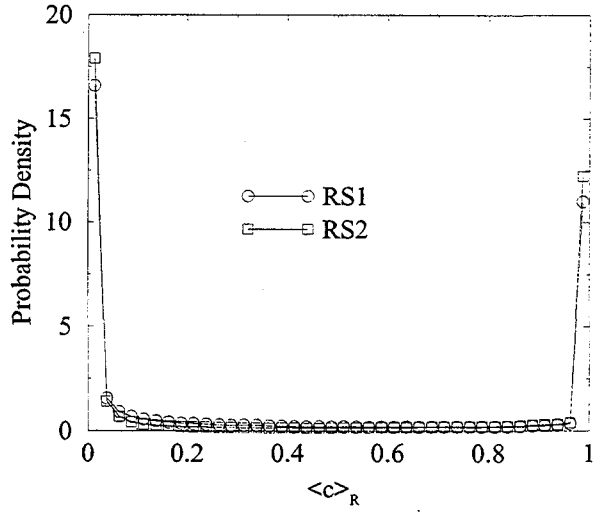

Fig. 8 Probability density of progress variable c.

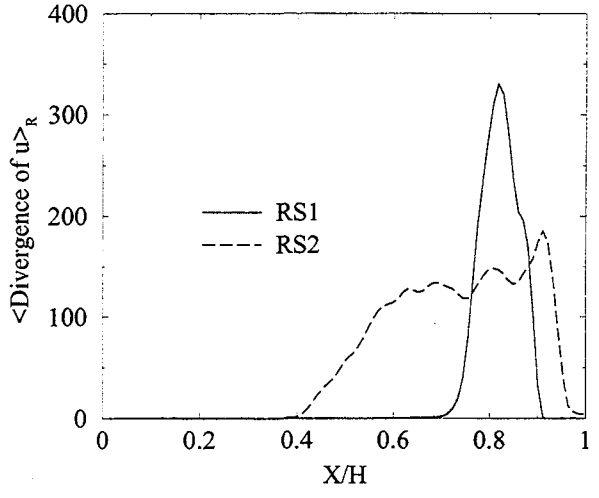

Fig. 7 Reynolds averaged divergence of velocity.

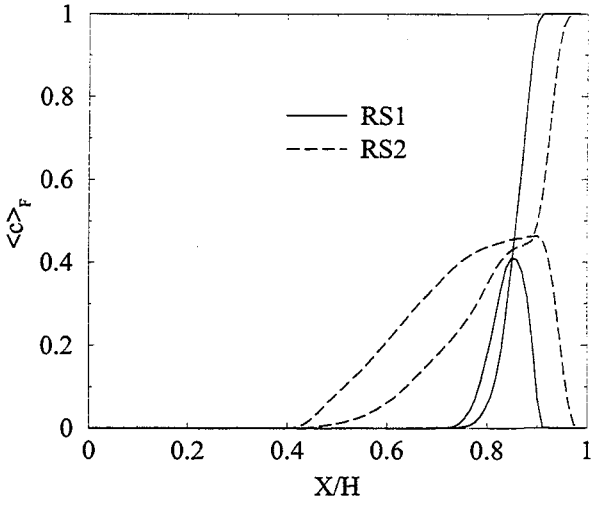

Fig. 9 Mean and r.m.s. progress variable c.

In summary, the analysis of the time averaged velocity data, suggest that the effect of heat release on the flow is significant at low u'/S_L and diminishes as u'/S_L increases. And as expected, the consumption rate is significantly increased by the increase in turbulence intensity. The flame structure is examined next.

In the beginning of this section it was stated that the G structure was resolved over five to seven cells making these simulated flames much thicker than their experimental counter parts. As the two-dimensional turbulence evolves the small scales quickly dissipate resulting in larger length scales at the flame zone than at the jet exit. Flamelet combustion is implicitly assumed by our choice of flamelet approach. To test whether the flamelet assumption is valid the probability density function (pdf) of the progress variable defined as $C = 1 - G$ is plotted as a function of the mean progress variable $< C >_R$ (where $<>_R$ denote Reynolds time averaging) in Fig. 8. In both cases, the pdf is bimodal which means that within the turbulent flame zone the progress variable is overwhelming either unreacted ($c = 0$) or fully reacted ($c = 1$). This result confirms that the flamelet assumption is valid for these conditions.

The flame brush is defined by the width of the average progress variable. This along with its variance for the two simulations are shown in Fig. 9. The flame brush for RS2 with twice the turbulence intensity is much broader than the RS1 flame brush as expected. In addition, it can be seen that the RS2 flame brush extends much further into the reactant flow and closer to the wall than does the RS1 flame.

The turbulent flux that appears as an unclosed term in the Favre averaged species equation is an important term that accounts for the turbulent diffusion of reacting scalars and must be modeled. It is common to assume a gradient diffusion model

$$\overline{\rho u'' c''} = \bar{\rho} \widetilde{u'' c''} = -\frac{\mu_t}{\sigma_c} \frac{\partial \tilde{c}}{\partial x_i} \qquad (6)$$

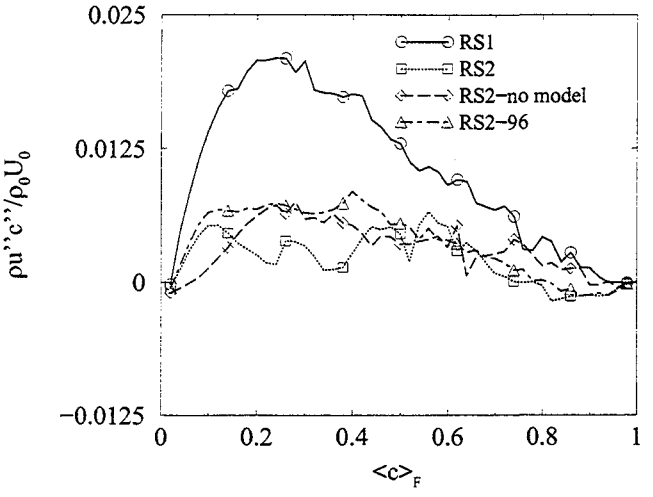

Fig. 10 Favre averaged turbulent scalar flux through the flame brush.

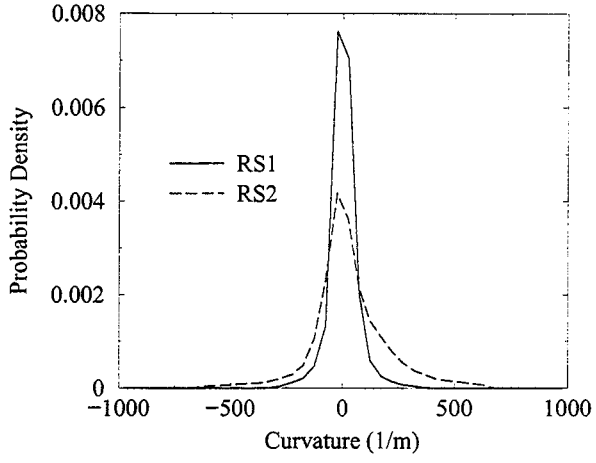

Fig. 11 Probability density of mean curvature.

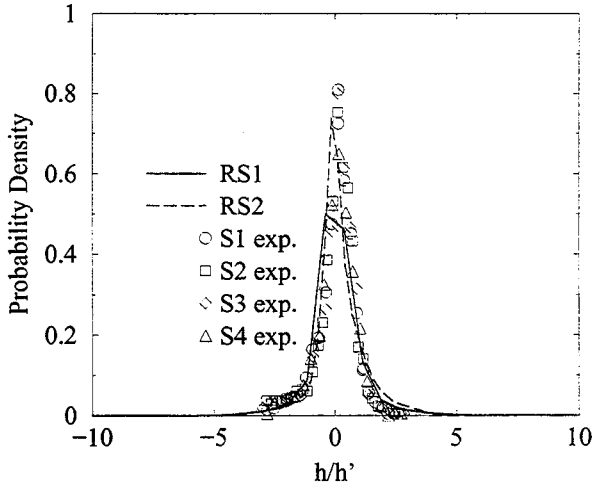

Fig. 12 Probability density of mean curvature normalized by the r.m.s. curvature compared to experimental data by Shepherd and Ashurst (1992).

where μ_t is an eddy viscosity, σ_c is the turbulent Schmidt number and x_i is a Cartesian coordinate component. The presence of counter-gradient diffusion in turbulent premixed combustion has been well established in theory (Libby and Bray, 1981), experiments (Cho *et al.*, 1988; Li *et al.*, 1996) and in direct numerical simulation (DNS) (Veynante and Poinsot 1997b; Veynante *et al.* 1997). The turbulent flux normalized by the reactant density (ρ_o) and the mean jet velocity (U_o) are shown in Fig. 10 plotted in progress variable space. In addition to RS1 and RS2, results from two other simulations are shown. The RS2-no model simulation was run with no subgrid models and RS2-96 was the same as RS2 except instead of resolving the jet with 64 points, 96 points were used. The turbulent flux is of counter-gradient type (+) for all four cases. By comparing the turbulent flux predicted in RS2, RS2-no model and RS2-96 it is apparent that the subgrid gradient diffusion model has a damping effect on the turbulent flux through the first half of the flame brush. This loss is compensated for by the increased resolution in RS2-96 which is to be expected because as the resolution increases, the subgrid model effects naturally diminish.

The curvature (h) distributions for RS1 and RS2 are shown in Fig. 11. The pdf for both simulations are symmetric with small mean values. An increase in turbulence intensity broadens the distribution by wrinkling the flame sheet more. The normalized distribustions are compared to the experimental data of Shepherd and Ashurst (1992) in Fig. 12, with all of their flames at $u'/S_L < 1$. The pdf of flame curvature collapses when normalized by the r.m.s. curvature (h'). The mean values of h are 4 and 35 and the r.m.s. curvatures are 65 and 175 for RS1 and RS2, respectively. The agreement between RS2 and the experiments is very close while the magnitude of the peak for RS1 is significantly lower, though the width of the distributions is in good agreement.

The normalized turbulent flame speed u_t/S_L, is plotted as a function of u'/S_L in Fig. 13. The turbulent flame speed is defined as the value of $< U >_R$ where the slope begins to change (Cho *et al.* 1986; Liu and Lenze, 1988). For zero heat release simulations, the value of $< U >_R$ is chosen where $< C >_R$ obtains a value of 0.02. This value was determined from averaging $< C >_R$ for the heat release cases once the location had been determined from where the slope changed. These two-dimensional simulations compare well with the data from Cho *et al.* (1986) but under predict the data of Liu and Lenze, (1988) significantly. The two higher S_L experiments of Liu and Lenze contain significant amounts of H_2 which is known to greatly enhance the turbulent flame speed through a dependence upon the Lewis number. The data by Cho *et al.* (1986) is for thermo-diffusively neutral flames. Since the G equation contains no Lewis number dependence it is resonable to expect better agreement with the data by

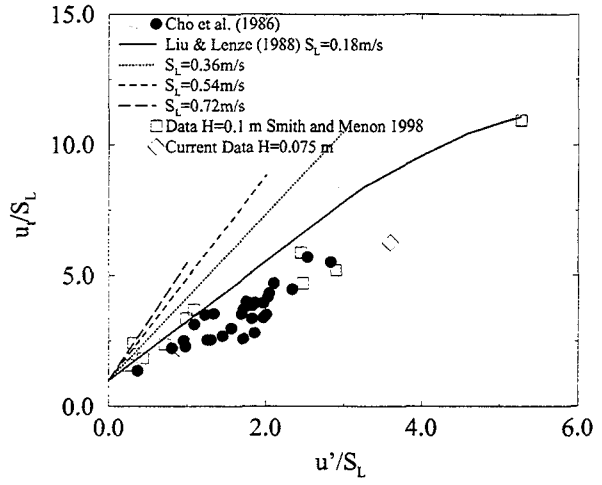

Fig. 13 Turbulent flame speed predictions compared with experimental data by Liu and Lenze 1986 and Cho *et al.* 1998.

Cho *et al.* (1986).

Based upon these results and results obtained earlier, the flamelet methodology has been shown capable of capturing large-scale flame/turbulence interactions which include the coupling of heat release to the hydrodynamic field, the increased burning rate caused by flame wrinkling and the turbulent transport of scalar fluxes. Therefore, the use of this method in practical applications where flamelet combustion can be assumed is justified. Large scale effects which include increased burning rate, unsteady heat release and transient flame propagation are well described using the G equation approach. However, in cases where flame stretch is important or thermo-diffusive effects this approach must be significantly modified.

Conclusions

A flamelet model for simulation of unsteady premixed flame propagation based on the G equation has been developed and applied to stagnation point flames. The filtered G equation which appears in the context of large-eddy simulations is closed using a gradient diffusion model for the unresolved scalar transport and a flame wrinkling model for the propagation term. The effects of significant heat release on the turbulent flow and the effect of varying turbulence intensity on the flame structure have been studied. The results show that at low turbulence intensities, the heat release dramatically alters the flow field and as the intensity is increased, heat release has a dimishing effect.

Acknowledgements

This work was supported in part by the Air Force Office of Scientific Research under the Focused Research Initiative, monitored by General Electric Aircraft Engines, Cincinnati, Ohio. Support for the computations was provided by the Navo HPC and the Pittsburgh Super Computing Center throurgh NSF and is gratefully acknowledged.

References

Bray, K. N. C. (1995) "Turbulent Transport in Flames," *Proc. R. Soc. Lond.* **A**, Vol. 451, pp. 231-256.

Cho, P., Law, C. K., Hertzberg, J. R. and Cheng, R. K. (1986) "Structure and Propagation of Turbulent Premixed Flames Stabilized in a Stagnation Flow," *Twenty-first Symposium (International) on Combustion*, The Combustion Institute, Pittsburgh, pp. 1493-1499.

Cho, P., Law, C. K., Cheng, R. K. and Shepherd, I. G. (1988) "Velocity and Scalar Fields of Turbulent Premixed Flames in Stagnation Flow," *Twenty-Second Symposium (International) on Combustion*, The Combustion Institute, Pittsburgh, pp. 739-745.

Im, H. G. (1995) "Study of turbulent premixed flame propagation using a laminar flamelet model," *Center For Turbulent Research, Annual Research Briefs*, pp. 347-360.

Im, H. G. Lund,T. S. and Ferziger, J. H. (1997) "Large Eddy Simulation of Turbulent Front Propagation With Dynamic Subgrid Models," *Phys. of Fluids*, Vol. 9, no. 12., pp. 3826-3833.

Kerstein, A. R. (1991) "Linear-Eddy Modeling of Turbulent Transport. Part 6. Microstructure of Diffusive Scalar Mixing Fields," *J. Fluid Mech.*, Vol. 231, pp. 361-394.

Kerstein, A. R., Ashurst, Wm. T. and Williams, F. A. (1988) The Field Equation for interface Propagation in an Unsteady Homogeneous Flow Field, *Phys. Rev.* A. 37, pp. 2728-2731.

Kerstein, A. R. (1986) "Pair-Exchange Model of Turbulent Premixed Flame Propagation," *Twenty-first Symposium (International) on Combustion*, The Combustion Institute, Pittsburgh, pp. 1281-1289.

Lee, S., Lele, S. K. and Moin, P. (1992) "Simulation of spatially evolving turbulence and the applicability of Taylor's Hypothesis in compressible flow," *Phys. of Fluids* A, Vol. 4, pp. 1521-1530.

Liu, Y. and Lenze, B. (1988) "The Influence of Turbulence on the Burning Velocity of Premixed $CH_4 - H_2$ Flames with Different Laminar Burning Velocities," *Twenty-Second Symposium (International) on Combustion*, The Combustion Institute, Pittsburgh, pp.

747-754.

McMurtry, P. A., Riley, J. J. and Metcalfe, R. W. (1989) "Effects of Heat Release on the Large-Scale Structure in Turbulent Mixing Layers," *J. Fluid Mech.*, Vol. 199, pp. 297-332.

Menon, S., McMurtry, P. A. and Kerstein, A. R. (1994) "A Linear Eddy Subgrid Model for Turbulent Combustion: Application to Premixed Combustion," Presented at the 31st Aerospace Sciences Meeting, Reno, Nv, January 11-14, AIAA-94-0107.

Menon, S. and Kerstein, A. R. (1992) "Stochastic Simulation of the Structure and Propagation Rate of Turbulent Premixed Flames," *Twenty-Fourth Symposium (International) on Combustion*, The Combustion Institute, Pittsburgh, pp. 443-450.

Menon, S. (1991) "Active Control of Combustion Instability in a Ramjet Using Large-Eddy Simulations," AIAA-91-0411, 29th Aerospace Sciences Meeting, Reno, Nv, January 7-10.

Menon, S. and Jou, W.H. (1991) Large-Eddy Simulations of Combustion Instability in an Axisymmetric Ramjet Combustor, *Combust. Sci. and Tech.*, Vol. 75, pp. 53-72.

Peters, N. (1986) "Laminar Flamelet Concepts in Turbulent Combustion," *Twenty-First Symposium (International) on Combustion*, The Combustion Institute, Pittsburgh, PA, pp. 1231-1250.

Peters, N. (1997) The Turbulent Burning Velocity for Large Scale and Small Scale Turbulence," *To be submitted to J. Fluid Mech.*.

Piana, J., Durcros, F. and Veynante, D. (1997) "Large Eddy Simulations of Turbulent Premixed Flames Bases on the G-Equation and a Flame Front Wrinkling Description," *11th Symposium on Turbulent Shear Flows*, Grenoble France.

Roberts W. L. and Driscoll J. F. and Drake M. C. and Goss L. P. (1993) "Images of the Quenching of a Flame by a Vortex-To Quantify Regimes of Turbulent Combustion," Combustion and Flame, vol. 94, pp. 58-69.

Smith, T. and Menon, S. (1998) "Subgrid Combustion Modeling for Premixed Turbulent Reacting Flows," AIAA-98-0242, 36th AIAA Aerospace Sciences Meeting and Exhibit, Reno, NV, January 6-10.

Smith, T. and Menon, S. (1997) "Large-Eddy Simulations of Turbulent Reacting Stagnation Point Flows," AIAA-97-0372, 35th AIAA Aerospace Sciences Meeting and Exhibit, Reno, NV, January 6-10.

Veynante, D., Trouvé , A., Bray, K. N. C. and Mantel, T. (1997) "Gradient and Counter-Gradient Scalar Transport in Turbulent Premixed Flames," *J. Fluid Mech.*, Vol. 332., pp. 263-293.

Veynante, D. and Poinsot, T. (1997a) "Large Eddy Simulation of Combustion Instabilities in Turbulent Premixed Burners," *Center for Turbulence Research, Annual Research Briefs*, pp. 253-274.

Veynante, D. and Poinsot, T. (1997b) "Effects of Pressure Gradients on Turbulent Premixed Flames," *J. Fluid Mech.*, pp. 83-114.

Williams, F. A. (1985) "Turbulent Combustion," *In The Mathematics of Combustion*, Ed. Buckmaster, J. D., Society for Industrial and Applied Mathematics, pp 97-131.

Yakhot, V. (1988) Propagation Velocity of Premixed Turbulent Flames, *Combust. Sci. Tech.*, 60, pp. 191-214.